Green Chemistry

PAPER

View Article Online
View Journal | View Issue

Cite this: *Green Chem.*, 2021, **23**, 1041

Copper anchored on phosphorus g-C_3N_4 as a highly efficient photocatalyst for the synthesis of *N*-arylpyridin-2-amines†‡

Jia-Qi Di, Mo Zhang, Yu-Xuan Chen, Jin-Xin Wang, Shan-Shan Geng, Jia-Qi Tang and Zhan-Hui Zhang *

Received 9th October 2020,
Accepted 4th January 2021

DOI: 10.1039/d0gc03400b

rsc.li/greenchem

A heterogeneous photocatalyst based on copper modified phosphorus doped g-C_3N_4 (Cu/P-CN) has been prepared and characterized. This recyclable catalyst exhibited high photocatalytic activity for the synthesis of *N*-arylpyridin-2-amine derivatives by the reaction of 2-aminopyridine and aryl boronic acid at room temperature under the irradiation of blue light. Importantly, the range of substrates for this coupling reaction has been expanded to include aryl boronic acids with strong electron-withdrawing groups as viable raw materials. In addition, this heterogeneous catalyst can be used at least 6 times while maintaining its catalytic activity.

Introduction

Amines and their derivatives are core structural motifs widely found in medicinal chemistry, materials science, and catalysis. Given the preeminence of aromatic and heteroaromatic amines, a plethora of methods have been developed for the synthesis of these compounds by using various named reactions, primarily from aryl halides and boronic acids, for example, Chan–Evans–Lam (CEL) reaction,[1–4] Ullmann–Goldberg coupling,[5,6] and Buchwald–Hartwig amination.[7–9] Among them, transition metal-catalyzed Chan–Evans–Lam oxidative coupling of aryl boronic acids and nitrogen nucleophiles to synthesize secondary aromatic amines in the presence of various oxidants is one of the most important transformations, which has attracted huge attention in the past decade. Most of the methods require the use of transition metal catalysts, ligands, and/or extreme conditions (high temperature, high pressure, strong oxidants, *etc.*), which ultimately result in reduced sustainability and a limited substrate range. In particular, aryl boronic acids with electron-withdrawing substituted groups are found to be poor substrates (Scheme 1a).[10–12] In 2016, Watson developed effective reaction conditions for the Chan–Evans–Lam amination of boronic acid pinacol (BPin) esters with alkyl and arylamines. Particularly, these conditions work effectively for the coupling of alkylamines (Scheme 1b).[13] In 2018, Schaper and co-workers

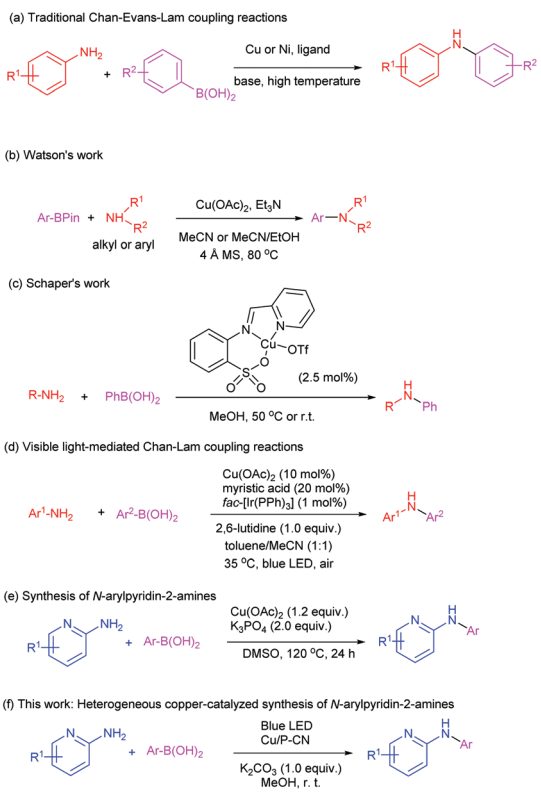

Scheme 1 Previous work and present reaction design.

Hebei Key Laboratory of Organic Functional Molecules, National Demonstration Center for Experimental Chemistry Education, College of Chemistry and Material Science, Hebei Normal University, Shijiazhuang, 050024, China.
E-mail: zhanhui@mail.nankai.edu.cn, zhanhui@hebtu.edu.cn

†Electronic supplementary information (ESI) available. See DOI: 10.1039/d0gc03400b

‡Dedicated to the 100th anniversary of Chemistry at Nankai University.

developed an efficient protocol by using copper(II) pyridyliminoarylsulfonate complexes with chloride or triflate counteranions as catalysts in Chan–Evans–Lam couplings, which avoids common side reactions such as deboration and homocoupling (Scheme 1c).[14] In addition, Kobayashi and co-workers established a procedure for the visible light-mediated Chan–Lam coupling reaction starting from aniline derivatives and arylboronic acids (Scheme 1d).[15] Through the effective combination of copper and photoredox catalysis, the substrate range of the oxidative coupling reaction is expanded to include electron-deficient aryl boronic acid as a viable starting material. Pyridine-containing amines are also a basic value-added unit in organic synthesis and have widespread applications in pharmaceutical science, material preparation, and anti-viral/anti-bacterial natural products.[16–19] Chen and co-workers developed a practical protocol for the preparation of these compounds *via* *N*-arylation of 2-aminopyridine with aryl boronic acids (Scheme 1e).[20] This protocol has several disadvantages such as utilizing an excessive amount of unrecoverable catalyst, running at high temperature, and very limited substrate scope. From the perspective of green and sustainable chemistry, it is still greatly desirable to develop novel catalytic materials to resolve the above issues.

Recently, due to the inexhaustible availability of light as clean energy, visible-light-induced photo-redox catalysis has emerged as an environmentally benign and powerful synthetic strategy for the development of new and valuable chemical transformations.[21–23] Most photo-redox processes use precious Ru and Ir-based polypyridyl photoredox catalysts.[24–26] As a low-cost alternative, organic dyes are also often used, but they usually have lower light stability.[27–29] Copper-based photocatalysts are rapidly emerging, which provide not only economic and ecological advantages, but also offer inaccessible inner-sphere mechanisms that have been successfully applied to challenging transformations.[30–35] Moreover, the combination of conventional photocatalysts and copper salts has emerged as an effective dual catalytic system for cross-coupling reactions.[36–38] On the other hand, heterogeneous catalysts are favored by industries because of their high efficiency and easy recycling. Consequently, some heterogeneous photocatalytic systems based on Cu have been developed.[39] Besides, polymeric graphitic carbon nitride (g-C_3N_4) has gained more attention as an excellent support to stabilize a metal catalyst for heterogeneous catalysis. Moreover, low-cost g-C_3N_4-based catalysts are easy to synthesize and separate from reaction mixtures, thereby facilitating repeated use of the catalyst.[40–44] The material is endowed with great many perfections such as high thermal and physicochemical stability, appropriate band gap energy and position (2.7 eV), and a unique electronic and surface structure. In addition, it has been known that when metallic elements were incorporated onto the g-C_3N_4 matrix, delocalized electrons are generated. Particularly, phosphorus-doped g-C_3N_4 (P-CN) can enhance the photocatalytic performance due to its relatively narrow band gap, stronger visible light response, larger specific surface area and higher charge carrier separation rate.[45–47]

Based on these backgrounds and our research group's persistent interest in the development of environmentally friendly synthetic methodologies,[48] herein, we report on the preparation of new phosphorus doped g-C_3N_4 (Cu/P-CN) and its application as a photocatalyst for the synthesis of *N*-arylpyridin-2-amine derivatives by the reaction of 2-aminopyridine and aryl boronic acid at room temperature under the irradiation of blue light (Scheme 1f).

Results and discussion

Following a modified reported method,[49] the Cu/g-C_3N_4 catalyst was synthesized: typically, $CuCl_2{\cdot}2H_2O$ was dispersed in methanol and sonicated. Then melamine was slowly added to the above solution. The resulting mixture was then refluxed at 65 °C for 3 h. The resulting precipitate was collected by filtration and dried in an oven at 70 °C. The solid was transferred to a ceramic crucible and calcined in a muffle furnace at 520 °C under a N_2 atmosphere. After cooling to room temperature, the final solid product (Cu-doped C_3N_4) was collected without further purification. Copper modified phosphorus doped g-C_3N_4 (Cu/P-CN) was prepared by mixing Cu/C_3N_4 with sodium hypophosphite ($NaH_2PO_2{\cdot}H_2O$).[50,52] The mixture was placed in a covered ceramic crucible and calcined at 300 °C for 2 h under a N_2 atmosphere. The obtained solid product was collected and washed with distilled water and ethanol, then dried in a vacuum oven at 80 °C for 24 h.

The X-ray photoelectron spectroscopy (XPS) patterns of Cu/P-CN are shown in Fig. 1. The XPS survey shows that copper, carbon, nitrogen, oxygen and phosphorus are detectable on the external surface of Cu/P-CN materials. The narrow scan for the Cu 2p (Fig. 1a) spectrum exhibited two main peaks at 935.5 and 955.0 eV. These peaks were attributed to the Cu $2p_{3/2}$ and Cu $2p_{1/2}$ orbitals, respectively, which indicates the presence of the Cu^{2+} moiety in the sample. The shift might result from the strong interaction between the Cu^{2+} species and P-CN. The C 1s at 288.4 eV and N 1s at 402.2 eV are assigned to the sp^2 C=N bond in the tri-*s*-triazine structure. The peaks at 288.4 eV and 284.5 eV in the C 1s zone are attributed to the electrons originating from the sp^2 C atom attached to an NH_2 group and to an aromatic carbon atom.[50] The peak of P 2p is located at 133.6 eV, indicating the presence of P on the Cu/P-CN material.[45]

The Cu/P-CN and the corresponding supporter g-C_3N_4 were characterized by powder X-ray diffraction (XRD). As shown in Fig. 2, the characteristic (002) interlayer stacking peak (27.6°) and the weak (100) diffraction peak (13.2°) of pure g-C_3N_4 (JCPDS no. 85-1326) were maintained in the Cu/P-CN material, suggesting that the structure of g-C_3N_4 did not change when the copper species were doped.

The morphology and microstructure of the samples were characterized *via* SEM and TEM. As depicted in Fig. 3a, it can be seen from the SEM image that Cu/C_3N_4 maintains the layered structure of C_3N_4. The introduction of Cu and P did not significantly change the structure of C_3N_4 (Fig. 3b). At the

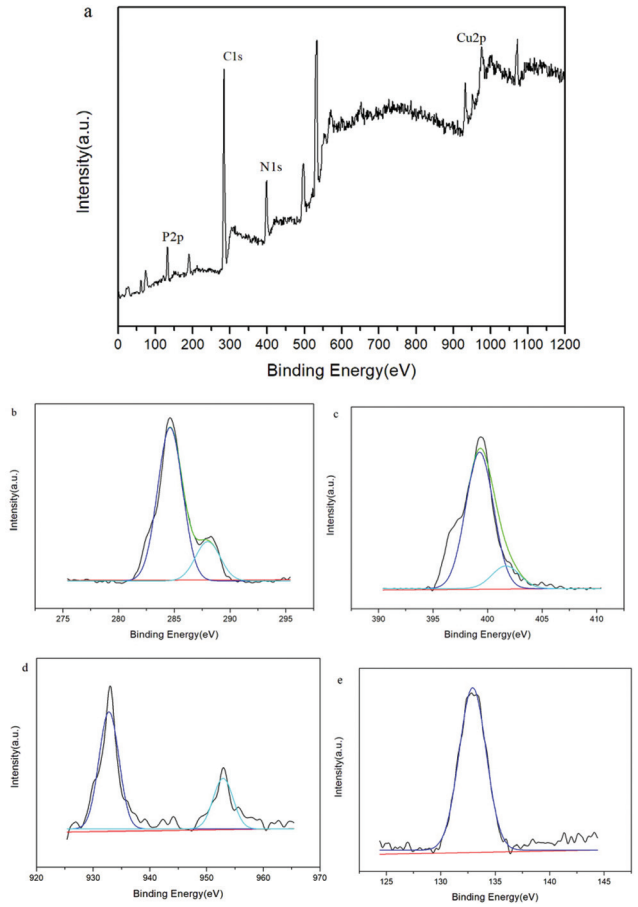

Fig. 1 XPS spectra of Cu/P-CN with (a) general scan, (b) C 1s, (c) N 1s and (d) Cu 2p, and (e) P 2p narrow scans.

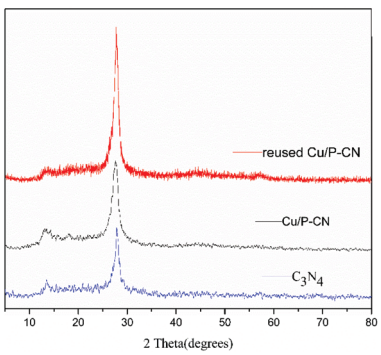

Fig. 2 XRD patterns of C_3N_4, Cu/C_3N_4 and Cu/P-CN.

same time, the corresponding energy-dispersive X-ray (EDX) spectrum of Cu/P-CN demonstrated the presence of C, N, Cu, and P (Fig. 4). The Cu/P-CN energy dispersive spectroscopy (EDS) elemental mapping was performed to determine the distribution pattern of the constituent elements. As shown in Fig. 4, all four main elements (Cu, C, N, and P) are uniformly distributed in the layer structure of the Cu/P-CN sample. Also, in order to determine the accurate content of Cu in the catalyst, it was treated with concentrated HCl and HNO_3 (the ratio

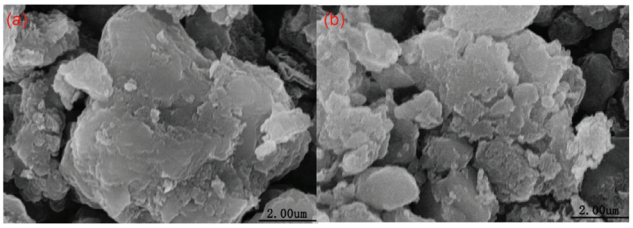

Fig. 3 SEM images of as-prepared samples (a) Cu/C_3N_4 and (b) Cu/P-CN.

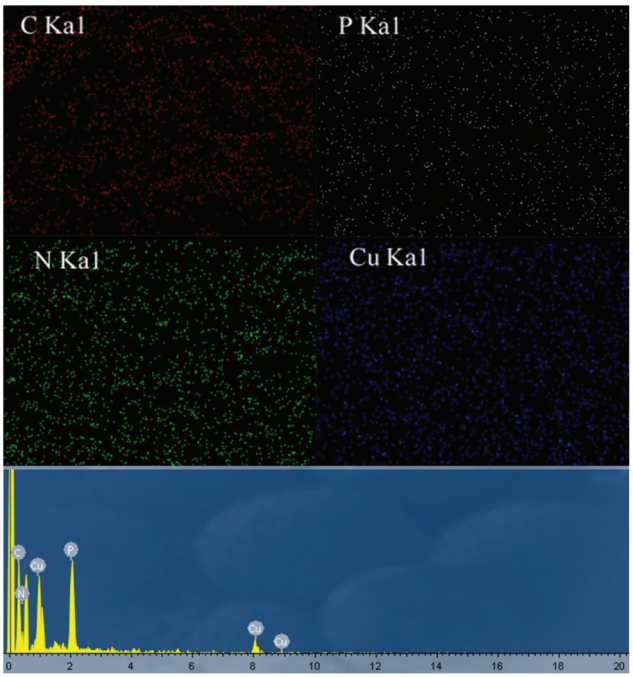

Fig. 4 EDS elemental mapping and EDX spectrum of Cu/P-CN.

of HCl to HNO_3 was 3/1) to digest the material and then analyzed by atomic absorption spectrometry (AAS) analysis. The Cu content was found to be 9.16%. The TEM image of Cu/P-CN further illustrates that the layered structure is still maintained after Cu loading (Fig. 5).

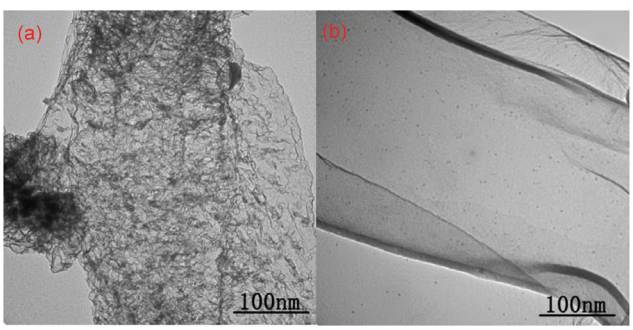

Fig. 5 TEM images of as-prepared samples (a) Cu/C_3N_4 and (b) Cu/P-CN.

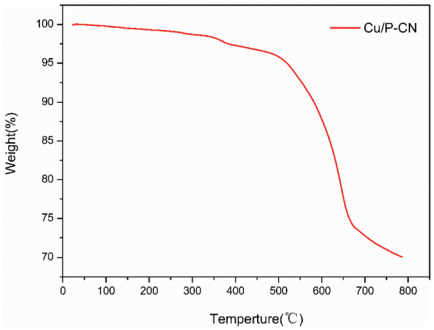

Fig. 6 TGA images of Cu/P-CN.

The thermal stability of Cu/P-CN was evaluated by thermogravimetric analysis (TGA) under a nitrogen atmosphere at a heating rate of 10 °C min^{-1} (Fig. 6). It was clear from the figures that there was a little mass loss below 100 °C due to the removal of adsorbed water, and further heating showed a slight weight loss of up to 550 °C. At this temperature, the tri-*s*-triazine structure decomposes, resulting in the total degradation of the carbon nitride matrix.

The specific surface area of the catalyst was measured by the nitrogen adsorption–desorption isotherm experiment (Fig. 7). The BET specific surface area of C_3N_4 and Cu/P-CN was calculated to be 29.0 m^2 g^{-1} and 14.0 m^2 g^{-1}, respectively.

To survey the catalytic activity of the prepared catalyst, we used simple pyridin-2-amine (1 mmol) and easily available phenylboronic acid (1 mmol) as model reactants, with K_2CO_3 as a base under irradiation with a blue-light-emitting diode (LED). As illustrated in Table 1, various solvents including H_2O, $CHCl_3$, ethyl lactate (EL), *N*,*N*-dimethylformamide (DMF), ethanol, acetonitrile, and methanol were screened. Only a trace amount of the desired product was observed when the reaction was carried out in H_2O (Table 1, entry 1). Among them, methanol gave the best result for achieving a maximum yield of product **3a**. The choice of the base also significantly affects the success of the reaction, and to our delight, cheap

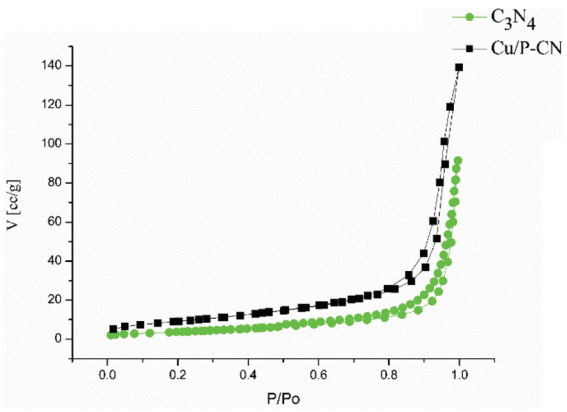

Fig. 7 N_2 adsorption–desorption isotherms of as-prepared C_3N_4 and Cu/P-CN.

Table 1 Reaction of pyridin-2-amine and phenylboronic acid under different reaction conditions[a]

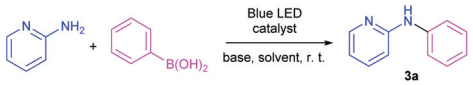

Entry	Catalyst	Solvent	Base	Time (h)	Yield[b] (%)
1	Cu/P-CN	H_2O	K_2CO_3	8	Trace
2	Cu/P-CN	$CHCl_3$	K_2CO_3	8	62
3	Cu/P-CN	EL	K_2CO_3	8	68
4	Cu/P-CN	DMF	K_2CO_3	8	72
5	Cu/P-CN	EtOH	K_2CO_3	8	77
6	Cu/P-CN	MeCN	K_2CO_3	8	83
7	Cu/P-CN	MeOH	K_2CO_3	8	95
8	Cu/P-CN	MeOH	Et_3N	8	53
9	Cu/P-CN	MeOH	Na_2CO_3	8	88
10	Cu/P-CN	MeOH	DBU	8	90
11	No	MeOH	K_2CO_3	12	0
12[c]	Cu/P-CN	MeOH	K_2CO_3	8	76
13[d]	Cu/P-CN	MeOH	K_2CO_3	8	82
14[e]	Cu/P-CN	MeOH	K_2CO_3	8	85
15[f]	Cu/P-CN	MeOH	K_2CO_3	8	95
16	C_3N_4	MeOH	K_2CO_3	12	0
17	Cu/C_3N_4	MeOH	K_2CO_3	8	90
18	$CuCl_2$	MeOH	K_2CO_3	8	17
19	Ni/P-CN	MeOH	K_2CO_3	8	26
20[g]	Cu/P-CN	MeOH	K_2CO_3	8	20
21[h]	Cu/P-CN	MeOH	K_2CO_3	8	Trace

[a] Reaction conditions: Pyridin-2-amine (1 mmol), phenylboronic acid (1 mmol), base (1 mmol), catalyst (0.2 mmol) in solvent (2 ml), room temperature, air, under blue light (455–460 nm) irradiation otherwise specified in the table. [b] Isolated yields. [c] Catalyst (0.05 mmol). [d] Catalyst (0.10 mol). [e] Catalyst (0.15 mmol). [f] Catalyst (0.25 mmol). [g] In the dark. [h] The reaction was carried out under a N_2 atmosphere.

K_2CO_3 outperformed all other bases tested. Further control experiments revealed that the reaction did not proceed in the absence of the catalyst (Table 1, entry 11). Decreasing the amount of the catalyst to 5 mol% reduced the yield to 76% (Table 1, entry 12). In contrast, the reaction yield was not improved when the amount of the catalyst was increased to 25 mol% (Table 1, entry 15). It is worth noting that expected product **3a** was not obtained when pure C_3N_4 was used as the catalyst. The use of Cu/C_3N_4 afforded inferior results compared to those using Cu/P-CN (Table 1, entry 17). Furthermore, as a more convincing comparison, the reaction can also be performed using pure $CuCl_2$, affording **3a** in 17% yield (Table 1, entry 18). A nickel anchored on phosphorus g-C_3N_4 (Ni/P-CN) was also used in place of Cu/P-C_3N_4 under otherwise identical conditions, targeted **3a** was formed only in 26% yield (Table 1, entry 19). Moreover, it was found that light plays a crucial role in the reaction, the yield of **3a** dropped significantly when the reaction was run in the absence of light (Table 1, entry 20). Notably, air is critical in this type of reaction, since only s trace amount of the product was obtained when the reaction was performed under a N_2 atmosphere (Table 1, entry 21).

With the establishment of the optimized reaction conditions, the substrate scope was investigated to probe the generality and identify the limitations of this Cu/P-CN catalyzed coupling reaction. As depicted briefly in Table 2, various sub-

Table 2 Substrate scope for the synthesis of *N*-arylpyridin-2-amines[a]

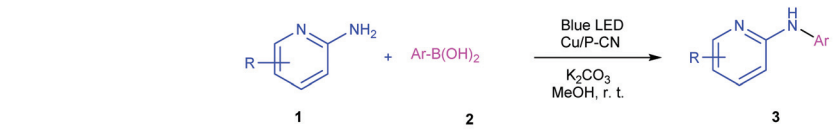

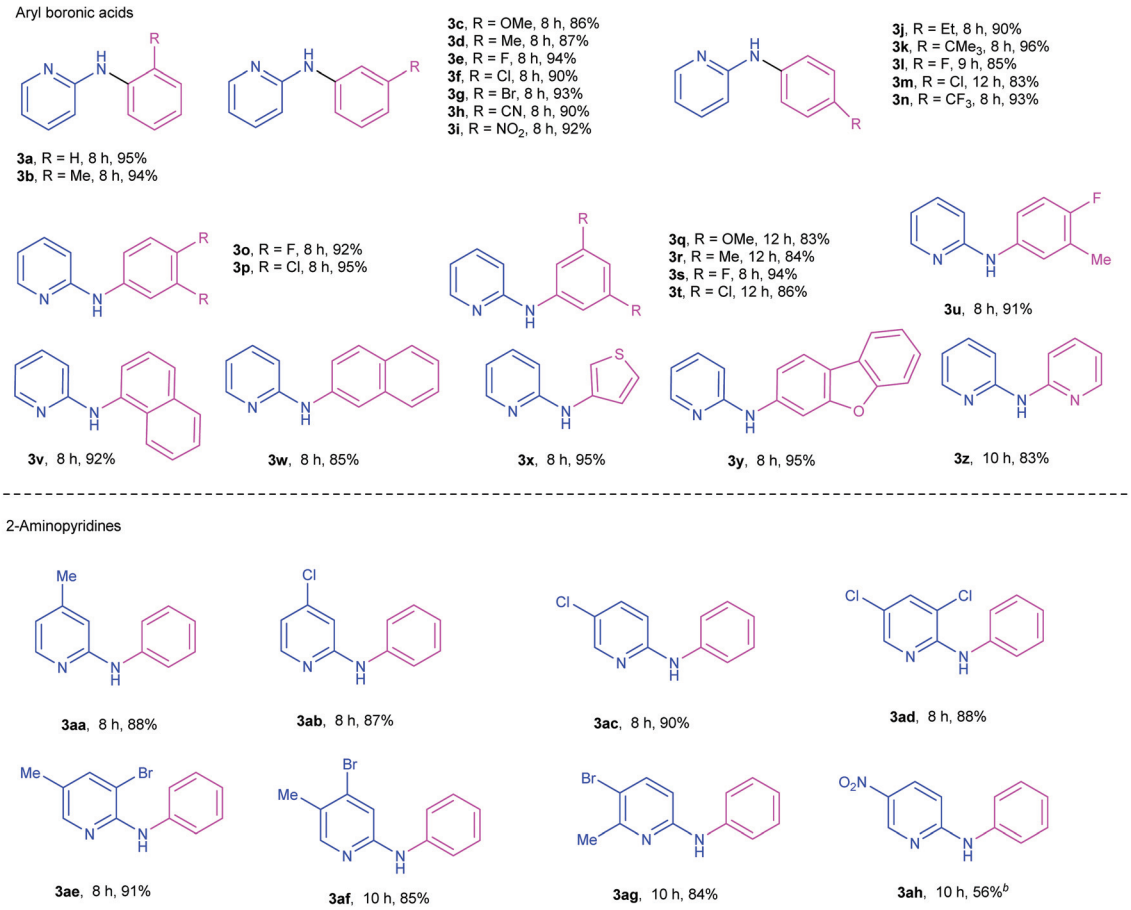

[a] Reaction conditions: Pyridin-2-amine (1 mmol), aryl boronic acid (1 mmol), K_2CO_3 (1 mmol), Cu/P-CN (0.2 mmol) in methanol (2 ml), room temperature, air, under blue light (455–460 nm, 10 W) irradiation, isolated yield. [b] The reaction was performed at 65 °C.

stituted phenylboronic acids bearing electron-rich groups (OMe, Et, Me and CMe_3), or electron-deficient groups (F, Cl, Br, CN and NO_2) at different positions were employed to the reaction with pyridin-2-amine under optimal conditions. To our delight, most of the reactions proceeded smoothly to afford the *N*-arylpyridin-2-amine derivatives in high yields. The above results demonstrated that substituents on the aromatic ring have no obvious effect on the yield. It is worth mentioning that the halogen group was all compatible with this reaction, which offered opportunities for downstream structural modification. Importantly, the strongly electron-withdrawing nitro group was tolerated and the corresponding product **3i** was obtained in 92% yield. The boronic acid with a larger aromatic group, such as naphthyl, also participated in the reaction, leading to the corresponding products **3v** and **3w** with high to excellent yields. The above conditions were also found to be suitable for heteroaryl substrates, such as thiophen-2-ylboronic acid, dibenzo[*b*,*d*]furan-3-ylboronic acid and pyridin-3-ylboronic acid, affording the potentially bio-important *N*-arylpyridin-2-amines **3x–3z** in high yields. Next, the reactions of phenylboronic acid with diversely substituted pyridin-2-amines were also examined. Substituted pyridin-2-amines with either electron-donating or weakly electron-withdrawing groups all gave excellent yields. 2-Aminopyridine with a strong electron-withdrawing group such as 5-nitropyridin-2-amine decreased the reactivity, and the reaction was performed at 65 °C to afford the desired product **3ah** in a moderate yield. To our disappointment, the reaction with secondary amines such as *N*-methylpyridin-2-amine and 6-methoxy-*N*-methylpyridin-2-amine did not afford the expected products.

Encouraged by the good performance of this protocol for *N*-arylpyridin-2-amines, coupling of conventional anilines

Scheme 2 Coupling of anilines bearing the strong electron-withdrawing group with phenylboronic acid.

bearing strong electron-withdrawing groups with aryl boronic acid are considered to be some of the biggest challenges in C–N bond formation *via* Chan–Evans–Lam.[10,14,51] Gratifyingly, 3-nitroaniline or 4-nitroaniline as the substrate reacted with phenylboronic acid to deliver the anticipated products **5a** and **5b** in high yields (Scheme 2).

To further showcase the synthetic utility of this method, a gram-scale experiment was also performed on the Cu/P-CN mediated model reaction. The reaction substrates were magnified 20 times, and the results showed that the reaction proceeded smoothly to afford the desired product **3a** without obvious erosion in the yield (Scheme 3).

According to the previous literature[15] and experimental observations, a tentative mechanism for this coupling reaction of 2-aminopyridine and aryl boronic acid is depicted in Scheme 4. Similar to the g-C_3N_4 photocatalyst that promotes organic photosynthesis,[52] upon irradiation with blue LED light, charge carriers of h^+ and e^- are generated on the surface of the P-CN photocatalyst. The photogenerated e^- could activate molecular O_2 into its reactive superoxide form ($O_2^{\bullet-}$). Singlet oxygen ($^1O_2$) could be formed through the oxidation of $O_2^{\bullet-}$ by photogenerated holes (h^+). The reactive oxygen species ($O_2^{\bullet-}$ and $^1O_2$) are confirmed by spin-trapping by electron paramagnetic resonance (EPR) experiments. When using 5,5-dimethyl-1-pyrroline *N*-oxide (DMPO) as a spin-trapping agent, a characteristic EPR signal of DMPO–$O_2^{\bullet-}$ is detected. Moreover, the formation of TEMP–$^1O_2$ has also been confirmed using 2,2,6,6-tetramethylpiperidine (TEMP) as a spin-trapping reagent, a characteristic 1 : 1 : 1 triplet EPR signal is observed (Fig. 8). These results indicate that $O_2^{\bullet-}$ coexists with $^1O_2$ in this photocatalytic oxidative reaction. Then, the oxidative coupling of 2-aminopyridine and aryl boronic acid occurs through several steps. Initially, the Cu(II) catalyst could undergo ligand exchange and transmetalation with 2-aminopyridine and phenylboronic acid to generate Cu(II) amide **A**. In the presence of $^1O_2$, Cu(II) is oxidized to Cu(III). Subsequently, the reduction and elimination reaction takes place to furnish the cross-coupling product **3a** and regenerated Cu(I). Then, Cu (I) is oxidized to Cu(II) by O_2 and the next cycle occurs.

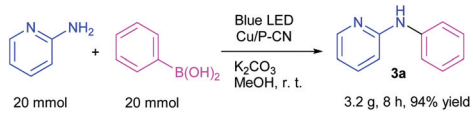

Scheme 3 A gram-scale experiment.

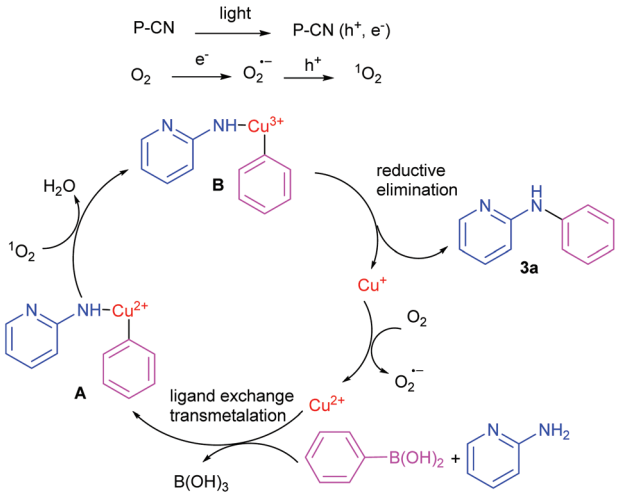

Scheme 4 Plausible catalytic cycle for the coupling reaction of pyridin-2-amine and phenylboronic acid.

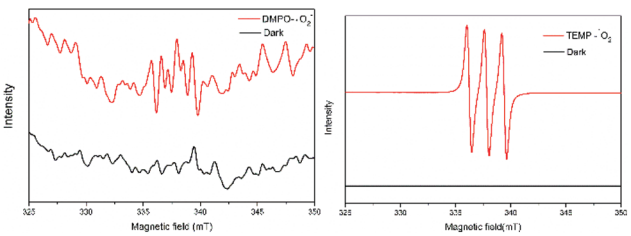

Fig. 8 EPR signals of the reaction solution in the dark (black line) and LED light illumination (red line) in the presence of DMPO (left) and TEMP (right) as spin-trapping reagents.

In order to determine the possibility of $^1O_2$ as the oxidant responsible for the oxidation of the copper catalyst, the model reaction was also performed in the presence of reagents known to interact with $^1O_2$ such as (*S*)-(−)-limonene, DL-α-tocopherol, and 1,1-diphenylethylene, and the results found that the reaction efficiency decreased dramatically. The mechanism described here is speculation and the actual pathway of this coupling reaction may be elucidated in due course.

Another basic ability to consider heterogeneous catalysts is the recyclability of the catalyst. Due to economic and environmental factors, easy separation is essential for industrial processes that reduce waste emissions and promote recyclability. In this study, the catalyst was separated by simple filtration, and recycling studies were performed for the reaction between pyridin-2-amine and phenylboronic acid under optimized conditions. After the reaction is complete, the catalyst is separated from the reaction mixture. The recovered catalyst is dried and then directly reused in the next round under the same reaction conditions. It can be seen from Fig. 9 that the reaction was repeated up to six times, and no significant changes in its catalytic activity were observed. The Cu leaching amount was also measured by inductively coupled plasma mass spectrometry (ICP-MS), and it was found that the Cu content after the sixth

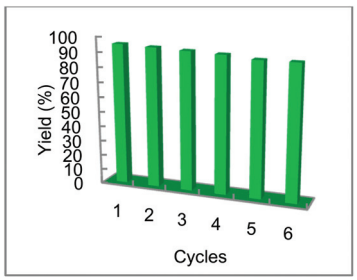

Fig. 9 Recycling of the catalyst.

cycle was 0.60 ppm. These results unambiguously demonstrate that the catalyst possesses excellent stability and robustness, and can be used many times in catalytic conversion.

Conclusions

In summary, a new heterogeneous photocatalyst was prepared and characterized using a variety of different techniques. Its catalytic performance for the cross-coupling between 2-aminopyridine and aryl boronic acid has been investigated. The catalyst showed high catalytic efficiency for the synthesis of diverse *N*-arylpyridin-2-amines. The synergistic effect of the dual-reactive polymer and copper nanoparticles enhances the catalytic activity and allows the reaction to proceed under mild conditions. The catalyst is separated by simple filtration and reused six times without significant loss in its catalytic activity and stability. The development of a more efficient and selective heterogeneous catalytic system and extension to other related organic synthesis are underway in our laboratory.

Experimental

General

All chemicals and reagents were obtained from commercial suppliers and used as received without further purification. The melting point was determined on an X-5 and was uncorrected. IR spectra were measured on a Bruker Tensor 27 Fourier transform infrared spectroscope using KBr disks. Powder X-ray diffraction data were obtained from a Bruker D8 Advance X-ray diffractometer, Cu-kα ray was used as the X-ray source, and the scanning rate was 0.05° s^{-1} between 20° and 80°. Transmission electron microscopy (TEM) was performed on a Hitachi H-7650 instrument running at 80 kV. Surface morphology was investigated using a Hitachi S-4800 SEM instrument. ^{1}H NMR and ^{13}C NMR data were acquired on Zhongke Niujin AS 400 spectrometer (400 MHz for ^{1}H NMR spectroscopy and 100 MHz for ^{13}C NMR spectroscopy) using TMS as the internal standard. Mass spectra were obtained on a 3200 QTRAP instrument with an ESI source. Thermogravimetric and thermal analyses were performed using a NETZSCH STA 449 F3 instrument at a heating rate of 10 K min^{-1} in a simulated air atmosphere. Inductively coupled plasma atomic emission spectroscopy analyses were performed with an X Series 2 spectrometer. A WP-VLH-1020 photoreactor from Xi'an WATTECS experimental equipment Co. Ltd was used for the irradiation experiment.

Synthesis of bulk g-C_3N_4. g-C_3N_4 is synthesized by simple calcination from melamine. Specifically, 10 g melamine is retained in a ceramic crucible and heated in a muffle furnace at 520 °C for 4 h under nitrogen. The light brown aggregates are ground into a powder using a mortar and pestle.

Synthesis of bulk Cu/C_3N_4. $CuCl_2{\cdot}2H_2O$ (5.1 g, 30 mmol) was dispersed in 200 mL of methanol and sonicated for 1 h to obtain a clear and transparent solution. Then melamine (4 g, 32 mmol) was added slowly to the above solution under stirring to prevent the formation of brown clumps. The resulting mixture was then refluxed at 65 °C for 3 h. After cooling to room temperature, the resulting precipitate was collected by filtration and dried in an oven at 70 °C. The solid was transferred to a ceramic crucible and then calcined in a muffle furnace at 520 °C for 4 h under N_2 at a heating rate of 10 °C min^{-1}. After cooling to room temperature, the solid product (Cu/C_3N_4) was collected without further purification.

Preparation of Cu modified phosphorus doped g-C_3N_4 (Cu/P-CN). Cu/P-CN was prepared by mixing Cu/C_3N_4 with $NaH_2PO_2{\cdot}H_2O$. In a typical experiment, the obtained Cu/C_3N_4 (300 mg) and $NaH_2PO_2{\cdot}H_2O$ (400 mg) were ground with a mortar and pestle. The uniform mixture was placed into a covered ceramic crucible and calcined at 300 °C for 2 h under a N_2 atmosphere. After completion of calcination and cooling to room temperature, the obtained solid product was collected and washed with distilled water and ethanol, and then dried in a vacuum oven at 80 °C for 24 h.

General procedure for the synthesis of *N*-arylpyridin-2-amines. In a 15 mL quartz tube equipped with a Teflon-coated magnetic stir bar, pyridine-2-amine (1 mmol), phenylboronic acid (1.0 mmol), K_2CO_3 (1 mmol) and Cu/P-CN (20 mol% Cu, 140 mg Cu/P-CN) were added successively in methanol (2 mL). The reaction tube was exposed to a blue LED (455–460 nm, 10 W) irradiation at a distance of approximately 3 mm from the bottom of the tube at room temperature in air with stirring for an appropriate time. The progress of the reaction was monitored by TLC. After completion of the reaction, the catalyst was separated by filtration. The mixture was diluted with H_2O and the product was extracted with EtOAc. The combined extracts were washed with brine and dried over Na_2SO_4. The solvent was removed, and the crude mixture was purified by flash column chromatography and eluted by hexane/EtOAc on silica gel to give the pure product. The recovered catalyst was washed with ethanol and ethyl acetate, dried in an oven and kept in a desiccator for further use.

Conflicts of interest

There are no conflicts to declare.

Acknowledgements

We are grateful for financial support from the National Natural Science Foundation of China (21272053), the Nature Science Foundation of Hebei Province (B2020205026), the Science Technology Research Foundation of Hebei Normal University (L2018Z06), Graduate Innovation Funding Program of Hebei Normal University (CXZZSS2020039) and the Undergraduate Training Programs for Innovation and Entrepreneurship (S202010094005).

Notes and references

1 (*a*) J. Q. Chen, J. H. Li and Z. B. Dong, *Adv. Synth. Catal.*, 2020, **362**, 3311–3331; (*b*) X. Liu and Z. B. Dong, *J. Org. Chem.*, 2019, **84**, 11524–11532; (*c*) J. Q. Chen, X. Liu, J. Guo and Z. B. Dong, *Eur. J. Org. Chem.*, 2020, 2414–2424.

2 (*a*) M. J. West, J. W. B. Fyfe, J. C. Vantourout and A. J. B. Watson, *Chem. Rev.*, 2019, **119**, 12491–12523; (*b*) J. C. Vantourout, L. Li, E. Bendito-Moll, S. Chabbra, K. Arrington, B. E. Bode, A. Isidro-Llobet, J. A. Kowalski, M. G. Nilson, K. M. P. Wheelhouse, J. L. Woodard, S. P. Xie, D. C. Leitch and A. J. B. Watson, *ACS Catal.*, 2018, **8**, 9560–9566; (*c*) C. G. McPherson, N. Caldwell, C. Jamieson, I. Simpson and A. J. B. Watson, *Org. Biomol. Chem.*, 2017, **15**, 3507–3518.

3 X. Y. Duan, N. Liu, J. Wang and J. Y. Ma, *Chin. J. Org. Chem.*, 2019, **39**, 661–667.

4 I. Munir, A. F. Zahoor, N. Rasool, S. A. R. Naqvi, K. M. Zia and R. Ahmad, *Mol. Diversity*, 2019, **23**, 215–259.

5 G. J. Sherborne, S. Adomeit, R. Menzel, J. Rabeah, A. Bruckner, M. R. Fielding, C. E. Willans and B. N. Nguyen, *Chem. Sci.*, 2017, **8**, 7203–7210.

6 G. Singh, M. Kumar and V. Bhalla, *Green Chem.*, 2018, **20**, 5346–5357.

7 R. Dorel, C. P. Grugel and A. M. Haydl, *Angew. Chem., Int. Ed.*, 2019, **58**, 17118–17129.

8 M. M. Heravi, Z. Kheilkordi, V. Zadsirjan, M. Heydari and M. Malmir, *J. Organomet. Chem.*, 2018, **861**, 17–104.

9 P. A. Forero-Cortes and A. M. Haydl, *Org. Process Res. Dev.*, 2019, **23**, 1478–1483.

10 N. Akatyev, M. Il'in, M. Ilin, S. Peregudova, A. Peregudov, A. Buyanovskaya, K. Kudryavtsev, A. Dubovik, V. Grinberg, V. Orlov, A. Pavlov, V. Novikov, I. Volkov and Y. Belokon, *ChemCatChem*, 2020, **12**, 3010–3021.

11 G. S. Astakhov, M. M. Levitsky, X. Bantreil, F. Lamaty, V. N. Khrustalev, Y. V. Zubavichus, P. V. Dorovatovskii, E. S. Shubina and A. N. Bilyachenko, *J. Organomet. Chem.*, 2020, **906**, 121022.

12 (*a*) V. H. Duparc and F. Schaper, *Organometallics*, 2017, **36**, 3053–3060; (*b*) A. C. Brewer, P. C. Hoffman, J. R. Martinelli, M. E. Kobierski, N. Mullane and D. Robbins, *Org. Process Res. Dev.*, 2019, **23**, 1484–1498.

13 J. C. Vantourout, R. P. Law, A. Isidro-Llobet, S. J. Atkinson and A. J. B. Watson, *J. Org. Chem.*, 2016, **81**, 3942–3950.

14 V. H. Duparc, G. L. Bano and F. Schaper, *ACS Catal.*, 2018, **8**, 7308–7325.

15 W. J. Yoo, T. Tsukamoto and S. Kobayashi, *Angew. Chem., Int. Ed.*, 2015, **54**, 6587–6590.

16 D. Zhou, H. Lee, J. M. Rothfuss, D. L. Chen, D. E. Ponde, M. J. Welch and R. H. Mach, *J. Med. Chem.*, 2009, **52**, 2443–2453.

17 J. M. Lapierre, S. Eathiraj, D. Vensel, Y. B. Liu, C. O. Bull, S. Cornell-Kennon, S. Iimura, E. W. Kelleher, D. E. Kizer, S. Koerner, S. Makhija, A. Matsuda, M. Moussa, N. Namdev, R. E. Savage, J. Szwaya, E. Volckova, N. Westlund, H. Wu and B. Schwartz, *J. Med. Chem.*, 2016, **59**, 6455–6469.

18 S. Patel, S. F. Harris, P. Gibbons, G. Deshmukh, A. Gustafson, T. Kellar, H. Lin, X. R. Liu, Y. Z. Liu, Y. C. Liu, C. Y. Ma, K. Scearce-Levie, A. S. Ghosh, Y. G. Shin, H. Solanoy, J. Wang, B. Wang, J. P. Yin, M. Siu and J. W. Lewcock, *J. Med. Chem.*, 2015, **58**, 8182–8199.

19 Z. J. Wu, K. L. Huang and Z. Z. Huang, *Org. Biomol. Chem.*, 2017, **15**, 4978–4983.

20 J. B. Chen, K. Natte, N. Y. T. Man, S. G. Stewart and X. F. Wu, *Tetrahedron Lett.*, 2015, **56**, 4843–4847.

21 (*a*) Q. Dou, C. J. Li and H. Y. Zeng, *Chem. Sci.*, 2020, **11**, 5740–5744; (*b*) L. Li, W. B. Liu, H. Y. Zeng, X. Y. Mu, G. Cosa, Z. T. Mi and C. J. Li, *J. Am. Chem. Soc.*, 2015, **137**, 8328–8331; (*c*) M. X. Liu, L. D. Tan, R. T. Rashid, Y. N. Cen, S. B. Cheng, G. Botton, Z. T. Mi and C. J. Li, *Chem. Sci.*, 2020, **11**, 7864–7870; (*d*) M. Zhang, M. N. Chen and Z. H. Zhang, *Adv. Synth. Catal.*, 2019, **361**, 5182–5190; (*e*) M. Zhang, Q. Y. Fu, G. Gao, H. Y. He, Y. Zhang, Y. S. Wu and Z. H. Zhang, *ACS Sustainable Chem. Eng.*, 2017, **5**, 6175–6182.

22 (*a*) U. Caudillo-Flores, D. Rodriguez-Padron, M. J. Munoz-Batista, A. Kubacka, R. Luque and M. Fernandez-Garcia, *Green Chem.*, 2020, **22**, 4975–4984; (*b*) J. Y. Dong, F. Y. Yue, W. T. Xu, H. J. Song, Y. X. Liu and Q. M. Wang, *Green Chem.*, 2020, **22**, 5599–5604; (*c*) M. Fu, X. C. Ji, Y. T. Li, G. J. Deng and H. W. Huang, *Green Chem.*, 2020, **22**, 5594–5598; (*d*) Q. Q. Kang, W. F. Wu, Q. Li and W. T. Wei, *Green Chem.*, 2020, **22**, 3060–3068; (*e*) L. L. Lu, Y. M. Li and X. F. Jiang, *Green Chem.*, 2020, **22**, 5989–5994; (*f*) M. R. Nadiveedhi, S. R. Cirandur and S. M. Akondi, *Green Chem.*, 2020, **22**, 5589–5593; (*g*) W. Zhao, C. X. Yang, J. D. Huang, X. L. Jin, Y. Deng, L. Wang, F. Y. Su, H. Q. Xie, P. K. Wong and L. Q. Ye, *Green Chem.*, 2020, **22**, 4884–4889; (*h*) X. X. Meng, Q. Q. Kang, J. Y. Zhang, Q. Li, W. T. Wei and W. M. He, *Green Chem.*, 2020, **22**, 1388–1392; (*i*) J. W. Zhou, L. M. Li, S. P. Wang, M. Yan and W. T. Wei, *Green Chem.*, 2020, **22**, 3421–3426.

23 (*a*) Y. L. Ban, J. L. Dai, X. L. Jin, Q. B. Zhang and Q. Liu, *Chem. Commun.*, 2019, **55**, 9701–9704; (*b*) W. Wei, L. L. Wang, H. L. Yue, P. L. Bao, W. W. Liu, C. S. Hu, D. S. Yang and H. Wang, *ACS Sustainable Chem. Eng.*, 2018, **6**, 17252–17257; (*c*) M. Zhang, W. Sun, H. Lv and Z.-H. Zhang, *Curr. Opin. Green. Sustain. Chem.*, 2021, **27**, 100390; (*d*) F. M. Wisser, M. Duguet, Q. Perrinet,

A. C. Ghosh, M. Alves-Favaro, Y. Mohr, C. Lorentz, E. A. Quadrelli, R. Palkovits, D. Farrusseng, C. Mellot-Draznieks, V. de Waele and J. M. Canivet, *Angew. Chem., Int. Ed.*, 2020, **59**, 5116–5122; (*e*) Q. Yu, Y. T. Zhang and J. P. Wan, *Green Chem.*, 2019, **21**, 3436–3441; (*f*) M. J. Cabrera-Afonso, S. Cembellín, A. Halima-Salem, M. Berton, L. Marzo, A. Miloudi, M. C. Maestro and J. Alemán, *Green Chem.*, 2020, **22**, 6792–6797.

24 M. Parasram and V. Gevorgyan, *Chem. Soc. Rev.*, 2017, **46**, 6227–6240.

25 C. K. Prier, D. A. Rankic and D. W. C. MacMillan, *Chem. Rev.*, 2013, **113**, 5322–5363.

26 (*a*) Q. Q. Zhou, Y. Q. Zou, L. Q. Lu and W. J. Xiao, *Angew. Chem., Int. Ed.*, 2019, **58**, 1586–1604; (*b*) M. Zhu, R. X. Li, Q. Q. You, W. J. Fu and W. S. Guo, *Asian J. Org. Chem.*, 2019, **8**, 2002–2005; (*c*) W. J. Fu, X. Han, M. Zhu, C. Xu, Z. Q. Wang, B. M. Ji, X. Q. Hao and M. P. Song, *Chem. Commun.*, 2016, **52**, 13413–13416; (*d*) M. Zhu, X. Han, W. J. Fu, Z. Q. Wang, B. M. Hao, X. Q. Hao, M. P. Song and C. Xu, *J. Org. Chem.*, 2016, **81**, 7282–7287; (*e*) H. M. Li, T. Y. Tu, X. Han, Z. Q. Wang, W. J. Fu, X. Q. Hao, M. P. Song and C. Xu, *Synlett*, 2018, 1729–1734; (*f*) Y. Gao, Y. Y. Liu and J. P. Wan, *J. Org. Chem.*, 2019, **84**, 2243–2251.

27 M. N. Chen, J. Q. Di, J. M. Li, L. P. Mo and Z. H. Zhang, *Tetrahedron*, 2020, **76**, 131059.

28 M. Xiang, C. Zhou, X. L. Yang, B. Chen, C. H. Tung and L. Z. Wu, *J. Org. Chem.*, 2020, **85**, 9080–9087.

29 Z. F. Li, H. Song, R. Guo, M. H. Zuo, C. F. Hou, S. N. Sun, X. He, Z. Z. Sun and W. Y. Chu, *Green Chem.*, 2019, **21**, 3602–3605.

30 V. P. Charpe, A. Sagadevan and K. C. Hwang, *Green Chem.*, 2020, **22**, 4426–4432.

31 K. X. Zhou, Y. Yu, Y. M. Lin, Y. J. Li and L. Gong, *Green Chem.*, 2020, **22**, 4597–4603.

32 C. J. Hunter, M. J. Boyd, G. D. May and R. Fimognari, *J. Org. Chem.*, 2020, **85**, 8732–8739.

33 V. K. K. Pampana, A. Sagadevan, A. Ragupathi and K. C. Hwang, *Green Chem.*, 2020, **22**, 1164–1170.

34 Y. Xiong and G. Z. Zhang, *Org. Lett.*, 2019, **21**, 7873–7877.

35 A. Hossain, A. Bhattacharyya and O. Reiser, *Science*, 2019, **364**, 450.

36 X. Y. Yu, J. Chen, H. W. Chen, W. J. Xiao and J. R. Chen, *Org. Lett.*, 2020, **22**, 2333–2338.

37 V. K. K. Pampana, A. Sagadevan, A. Ragupathi and K. C. Hwang, *Green Chem.*, 2020, **22**, 1164–1170.

38 Y. J. Zhang and D. Y. Zhang, *Org. Biomol. Chem.*, 2020, **18**, 4479–4483.

39 M. B. Gawande, A. Goswami, F. X. Felpin, T. Asefa, X. X. Huang, R. Silva, X. X. Zou, R. Zboril and R. S. Varma, *Chem. Rev.*, 2016, **116**, 3722–3811.

40 A. Savateev, I. Ghosh, B. Konig and M. Antonietti, *Angew. Chem., Int. Ed.*, 2018, **57**, 15936–15947.

41 L. L. Wang, M. Liu, W. Y. Zha, Y. C. Wei, X. F. Ma, C. W. Xu, C. G. Lu, N. F. Qin, L. Gao, W. Z. Qiu, R. J. Sa, X. Z. Fu and R. S. Yuan, *J. Catal.*, 2020, **389**, 533–543.

42 J. J. Li, Y. N. Chen, X. Yang, S. Y. Gao and R. Cao, *J. Catal.*, 2020, **381**, 579–589.

43 F. Verma, P. Shukla, S. R. Bhardiya, M. Singh, A. Rai and V. K. Rai, *Adv. Synth. Catal.*, 2019, **361**, 1247–1252.

44 H. Xu, K. Y. Wu, J. Tian, L. Zhu and X. Q. Yao, *Green Chem.*, 2018, **20**, 793–797.

45 L. B. Jiang, X. Z. Yuan, G. M. Zeng, X. H. Chen, Z. B. Wu, J. Liang, J. Zhang, H. Wang and H. Wang, *ACS Sustainable Chem. Eng.*, 2017, **5**, 5831–5841.

46 M. Bellardita, E. I. Garcia-Lopez, G. Marci, I. Krivtsov, J. R. Garcia and L. Palmisano, *Appl. Catal., B*, 2018, **220**, 222–233.

47 J. Q. Guo, Y. T. Wang, Y. H. Li, K. L. Lu, S. H. Liu, W. Wang and Y. Q. Zhang, *Adv. Synth. Catal.*, 2020, **362**, 3898–3904.

48 (*a*) G. Gao, J. Q. Di, H. Y. Zhang, L. P. Mo and Z. H. Zhang, *J. Catal.*, 2020, **387**, 39–46; (*b*) H. J. Wang, M. Zhang, W. J. Li, Y. Ni, J. Lin and Z. H. Zhang, *Adv. Synth. Catal.*, 2019, **361**, 5018–5024; (*c*) M. Zhang, Y. Han, J. L. Niu and Z. H. Zhang, *Adv. Synth. Catal.*, 2017, **359**, 3618–3625.

49 L. Muniandy, F. Adam, A. R. Mohamed, A. Iqbal and N. R. A. Rahman, *Appl. Surf. Sci.*, 2017, **398**, 43–55.

50 W. Liu, L. L. Cao, W. R. Cheng, Y. J. Cao, X. K. Liu, W. Zhang, X. L. Mou, L. L. Jin, X. S. Zheng, W. Che, Q. H. Liu, T. Yao and S. Q. Wei, *Angew. Chem., Int. Ed.*, 2017, **56**, 9312–9317.

51 Y. Han, M. Zhang, Y. Q. Zhang and Z. H. Zhang, *Green Chem.*, 2018, **20**, 4891–4900.

52 (*a*) A. Savateev, I. Ghosh, B. Köenig and M. Antonietti, *Angew. Chem., Int. Ed.*, 2018, **57**, 15936–15947; (*b*) Y. Zhao and M. Antonietti, *Angew. Chem., Int. Ed.*, 2017, **56**, 9336–9340; (*c*) F. Su, S. C. Mathew, L. Moehlmann, M. Antonietti, X. Wang and S. Blechert, *Angew. Chem., Int. Ed.*, 2011, **50**, 657–660.